A | R | J
Amrit Research Journal December 2022, Vol. 3, Issue 1, 29-45
ISSN: 2738-9553
RESEARCH ARTICLE

Shorea robusta Bark Extract as a Novel Green Inhibitor for Mild Steel Corrosion in 1 M H_2SO_4 Solution

Ajay Kumar Bajgai[1], Rajaram Karki[1], Jamuna Thapa Magar[1], Puspa Lal Homagai[1], Hari Bhakta Oli[1]*, Deval Prasad Bhattarai[1]*

[1]Department of Chemistry, Amrit Campus, Tribhuvan University, Kathmandu, Nepal.

**Corresponding Author: hari.oli@ac.tu.edu.np(HBO) and deval.bhattarai@ac.tu.edu.np(DPB)*

(Received: August 25, 2022, Received in revised form: November 21, Accepted: December 15, 2022, Available Online)

Highlights

- Methanol extract from *Shorea robusta* bark was used for corrosion inhibition
- Weight loss and electrochemical measurement methods were employed for the study of corrosion inhibition
- Electrochemical measurements reflected the mixed type of inhibition property
- Corrosion kinetics and thermodynamics of the corrosion were evaluated

Abstract

Extract of Shorea robusta bark as a novel green inhibitor for mild steel (MS) corrosion has been investigated. Qualitative chemical tests, UV, and FTIR measurements were carried out to confirm phytochemicals in the extract. Gravimetric as well as electrochemical methods were employed to examine the inhibition efficiency of the extract. Effects of inhibitor concentration, immersion time as well as working temperature were investigated by weight loss measurement method. Weight loss measurement reveals the maximum inhibition efficiency of 1000 ppm inhibitor for half an hour immersion time. Also, 1000 ppm inhibitor can work up to a temperature of 55 °C with 50% efficiency. Electrochemical measurements reflected the mixed type of inhibition behavior of the inhibitor. Polarization measurement results, the 93.73% and 75%, respectively for as-immersed and immersed samples in1000 ppm inhibitor concentration. Based on these findings, it is revealed that the Shorea robusta bark extract could be used as low temperature inhibitor.

Keywords: *Shorea robusta, extract, green inhibitors, mild steel, weight loss, polarization*.

Introduction

Corrosion is natural and can be controlled by the applications of inhibitors in various processes such as cleaning boilers, acid pickling and descaling [1,2]. An inhibitor is a chemical compound that when added in a trace amount to the corrosive media has a strong tendency to decrease the corrosion rate of the metallic materials. The manifestations of such inhibitory action generally occur through the quasi-substitution phenomenon i.e. simultaneous replacements of water molecules by the inhibitor species via the adsorption process on the metallic materials [3]. However, the effectiveness of inhibitors is partly dependent on the metals/alloys to be protected as well as the severity of the environment.

There are many compounds that are reported as corrosion inhibitors. Some of them are polymers [3–5], inorganic [6,7], and synthetic organic compounds [8,9]. However, due to their toxicity, non-biodegradability, expensiveness, and difficulty in the synthesis process limit their uses [10]. So, to overcome these limitations, the inhibitor with certain characteristic features such

*Corresponding author

as biodegradable, eco-friendly, easily available, heavy metals free, and ecologically acceptable green corrosion inhibitors are in focus [11]. So, more studies on the plant inhibitors for green corrosion chemistry are now on trend.

The application of natural products particularly the extracts obtained from leaves, fruits, seed, root, bark, flower and entire body of the plant are mostly used as green corrosion inhibitors [12]. Because they contain several phytochemicals with polar atoms, and electron rich hetero-atoms such as O, N, P, and S. These polar atoms have strong affinity towards interaction and adsorption onto the metal surface [13]. Phytochemicals like Alkaloid, Flavonoid, Imidazole, Glucose, Amino acids, Sarasapogenin, quinolone derivatives, thiourea derivatives, thiosemicarbazide, thiocyanates, saponins, and tannins, etc. [14,15] could take part in corrosion inhibition process.

Recently, research in the searching of green corrosion inhibitors are going on. Some of the reported inhibitors for mild steel corrosion with promising efficiency are tabulated in table 1.

Table 1. Extract of different plants as green corrosion inhibitor and their inhibition efficacy

S.N.	Plant	Plant parts	Phytochemicals	Electrolyte	Characterization	Efficiency (%)	Reference
1	*Artemisia vulgaris*	Stem	Alkaloids	1 M H_2SO_4	Weight loss Polarization	92.58 88.06	[1]
2	*Solanum tubersum*	Stem	Alkaloids	1 M H_2SO_4	Weight loss Polarization	90.79 83.22	[1]
3	*Coriaria nepalensis*	Stem	Alkaloids	1 M H_2SO_4	Weight loss Polarization	96.41 97.03	[2]
4	*Artemisia vulgaris*	Stem	Methanol Extract	1 M H_2SO_4	Weight loss	67	[10]
5	*Rhynchostylis retusa*	Rhizome	Alkaloids	1 M H_2SO_4	Weight loss Polarization	87.51 93.24	[13]
6	*Urtica dioica*	Leaves	Methanol Extract	1 M HCl	EIS Polarization Weight loss	92	[16]
7	*Gongronema latifolium*	Whole plant	Methanol Extract	0.5 M HCl	Weight loss	81.69	[17]
8	*Lantana camara*	Bark	Methanol Extract	1 M HCl	Polarization	97.33	[18]
9	*Lavandula mairei*	Whole plant	Methanol Extract	1 M HCl	EIS Polarization Weight loss	91.6 89.8 88.9	[19]
10	*Catharanthus roseu*	Whole plant	Methanol Extract	0..5M NaCl	Weight loss	82	[20]
11	*Laurus nobilis*	Whole plant	Methanol Extract	0..5M NaCl	Weight loss	65	[20]
12	*Areca catechu*	Whole plant	Methanol Extract	0..5M NaCl	Weight loss	50	[20]
13	*Green tea and black tea*	Leaves	Methanol Extract	1 M HCl	Weight loss	83.1 and 81.7	[21]
14	*Gmelina arborea*	Bark	Methanol extract	1 M HCl	Weight loss	96	[22]
15	*Hyptis suaveolens*	Leaves	Methanol Extract	1 M H_2SO_4	EIS Polarization Weight loss	93.3 95 76	[23]
16	*Pennisetum glaucum*	Seeds	Methanol Extract	1 M HCl 1M H_2SO_4	Polarization	91.42 91.17	[24]

17	*Mahonia nepalensis*	Stem	Barberine Molecule	1 M H_2SO_4	EIS Polarization Weight loss	98.02 98.19 97.2	[25]
18	*Equisetum hymale*	Whole plant	Methanol Extract	1 M H_2SO_4	Polarization EIS	92.74 82	[26]
19	*Caulerpa racemosa*	Alga	Alkaloids	1 M HCl	Weight loss Polarization EIS	83 80 85	[27]
20	*Ochrosia oppositifolia*	Bark and leaves	Alkaloids	1 M HCl	EIS Polarization	93 91	[28]
21	*Neolamarckia cadamba*	Bark and leaves	Alkaloids	1 M HCl	EIS Polarization	89 83	[29]
22	*Garcinia kola*	Seed	Alkaloids	5 M H_2SO_4	Weight loss	98	[30]
23	*Solanum melongena*	Leaves	Alkaloids	Sodium trioxocarbonate	Weight loss	81.1	[31]
24	*Geissospermum laeve*	Whole plant	Alkaloids	1 M HCl	EIS	92	[32]
25	*Retama monosperma*	Seed	Alkaloids	1 M HCl	EIS	94.4	[33]
26	*Rauvolfia macrophylla*	Bark	Alkaloids	0.5 M H_2SO_4 1 M HCl	Polarization, EIS Polarization, EIS	93, and 97 92, and 93	[34]
27	*Retama monosperma*	Seeds	Alkaloids	1 M HCl	DFT	94.42	[35]
28	*Alnus nepalensis*	Bark	Alkaloids	1 M H_2SO_4	Weight loss Polarization	71.94 78.48	[36]
29	*Acacia catechu*	Bark	Alkaloids	1 M H_2SO_4	Weight loss Polarization	93.96 98.54	[37]
30	*Solanum xanthocarpum*	Stem	Alkaloids	1 M H_2SO_4	Weight loss Polarization	93.14 98.14	[38]

These inhibitors are reported with good inhibition efficiency, however, researches are not limited up to these findings. Plant abundance, high inhibition efficacy, higher working temperature, and economy are still to be considered. The inhibition capability of the plant varies with the variation in the composition of phytochemical components which in turn differs in different plant species. So, this study aims to examine the corrosion inhibition property of the *Shorea robusta* bark extract.

Shorea robusta is the superabundant plant belonging to the family Dipterocarpaceae. The plant 'Saal' has radical distribution in western Terai of Nepal [39]. The stem of this plant is primarily used as timber while the bark is lost as waste biomass. It is reported that the bark extract of this plant contains many secondary metabolites [40,41] and large number of compounds: ursolic acid, a-amyrenone, a-amyrin, b-amyrin, shoreaphenol, etc.[41]. These compounds have large aromatic rings with π-electrons which are available as the active sites for adsorption. So, they may be considered as green alternative for corrosion inhibition.

Materials and Methods

Sample Collection and Preparation of Extract

The chemicals used to prepare extract are hexane (Qualigens, 98.99%, sp. gr. 0.66-0.67) and methanol (Fischer scientific, 99%, sp. gr. 0.79-0.793). *Shorea robusta* (SR) barks were collected from the forest of Bardiya District (Latitude: 28.27, Longitude:

81.53). The collected bark sample was washed with tap water to remove attached specks of dust and shade dried. The half dried bark sample was chopped into small pieces and left for 9 days to shade dried. Then the dried bark was ground into a fine powder. 100 g of powdered sample was soaked into 500 mL of hexane for 24 hours followed by filtration. The residue was soaked in 800 mL methanol for 24 h. The sample mixture was then kept in an ultrasonicator for about 1.5 h to intermix the extracting solvent and the bark powder to extract phytochemicals by the vibrations of ultrasonicator at molecular level. The mixture was then filtered and the filtrate was concentrated. The extraction process was repeated till the clear solution was observed. The concentrated filtrate was dried by evaporation by using Clifton water bath at temperature 40 °C and labeled as bark extract of SR. The overall process is presented in the scheme 1.

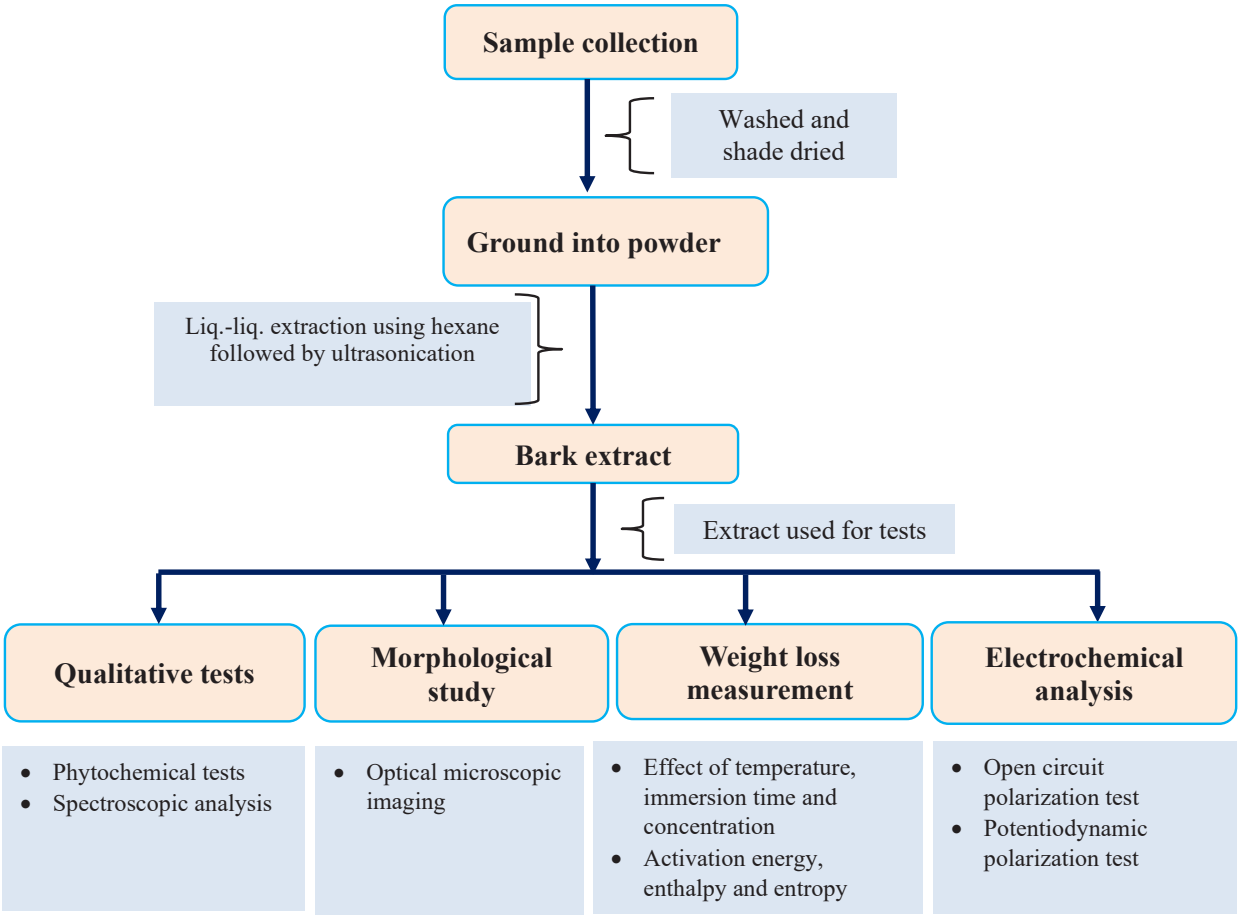

Scheme 1: Experimental Schematic

Qualitative tests of phytochemicals of *S. robusta*

Qualitative chemical test of different phytochemicals present in the methanol extract of *S. robusta* bark were carried out.

Fourier Transformed Infrared Spectroscopic Measurement

FTIR spectroscopy, a powerful tool, was used to identify the functional groups present in the organic compounds. FTIR spectrometric determination of extract was carried out at the Department of Chemistry, Amrit Campus, Kathmandu, Nepal. A spectrum of the methanol extract was recorded using Perkin Elmer Spectrometer 10.6.2 version. The background correction was carried out using isopropanol. All the spectral data were collected from 450-4000 cm^{-1} cutoff range with 4 cm^{-1} resolution.

Ultraviolet Visible Spectroscopic Measurement

The incident light of known energy subjected to the analyte matter is being adsorbed, reflected or transmitted. The absorbance of the light by the analyte solution across the ultraviolet and visible ranges is used to determine by Ultraviolet-visible (UV-Vis) spectrophotometry. This helps for the identification of unsaturation or presence of lone pair of electrons in the organic

compounds. The UV spectra of alkaloid have been recorded using a Labtronics, LT-2802 double beam UV-Vis spectrometer in Amrit Campus, Kathmandu, Nepal.

Corrosive and Inhibitor Medium Preparation

One molar sulphuric acid was used as corrosive medium which was prepared by diluting the required volume of concentrated H_2SO_4 (Fischer scientific, 97 %, sp. gr. 1.835 g/mL) in 1000 mL volumetric flask containing distilled water. The volume was maintained up to mark by adding distilled water. Similarly, the inhibitor stock solution was prepared by dissolving 1 g of extract in 1000 mL of 1M H_2SO_4. The mixture was filtered to remove the undissolved part. The volume of filtrate was then maintained 1000 mL by adding 1 M H_2SO_4 solution and labeled as stock solution. The required concentration of the inhibitor solutions: 200, 400, 600, and 800 ppm were prepared from this 1000 ppm of stock solution by serial dilution.

Mild Steel Sample Preparation

The mild steel (MS) coupons of dimension (4 × 4 × 0.2) cm^3 were taken from the local supplier, Kathmandu. Before experimenting, Silicon Carbide (SiC) paper of different grades (400, 600, 800, 1000, and 1200) was used to polish the mild steel, washed with hexane to remove organic impurities followed by sonication in ethanol. Previous to each experiment, the dimension of each coupon was measured by a digital vernier caliper.

Weight loss Experiment

The weight loss measurement method was applied to examine the corrosion by immersing the MS coupons into the acid solution in the absence and presence of different concentrations of inhibitors. While monitoring corrosion rate, the dimension of MS coupons were measured, and immersed in inhibitor solution of different concentrations (0, 200, 400, 600, 800, 1000 ppm) at a different time.

The weight of MS was measured by using a 4-digit weight balance (Phoenix instrument-PH2204C) before and after immersion tests into aggressive and inhibitor solutions. The inhibition efficiency was calculated using equations 1.

$$\text{Inhibition Efficiency} = \frac{\Delta W_a - \Delta W_p}{\Delta W_a} \times 100 \quad (1)$$

Where,

ΔW_a = Weight loss in absence of an inhibitor

ΔW_p = Weight loss in presence of an inhibitor

Electrochemical Measurement

In electrochemical measurement, the open circuit potential (OCP) and potentiodynamic polarization were carried out, and an electrochemical cell setup was arranged by taking MS coupon as a working electrode, graphite and saturated calomel electrode, respectively as counter electrode and reference electrode. The OCP measurement in different concentrations of inhibitor solutions was carried out for 30 minutes, before polarization measurement. The potentiodynamic polarization was carried out in the potential window -0.8 to -0.2 V i.e. ±300 mV from OCP in different concentrations of inhibitor for both immersed and as-immersed conditions. The inhibition efficiency of the inhibitor was calculated using equation 2.

$$\text{Inhibition efficiency (\%)} = \frac{i_a - i_p}{i_a} \times 100 \quad (2)$$

Where,

i_a = Corrosion current density in absence of an inhibitor

i_p = Corrosion current density in presence of an inhibitor

Results and Discussion

The characterization of extracted phytochemical was carried out by chemical tests, UV measurement, and FTIR spectroscopic measurements. The corrosion inhibitory behavior of the plant extract was studied by the weight-loss method, open circuit potential, and potentiodynamic polarization.

Qualitative tests of phytochemicals of *S. robusta*

Qualitative chemical test methods for the different phytochemicals in the methanol extract of *S. robusta* bark were performed in the laboratory are reported in table 2.

Table 2. Phytochemical screenings of the Methanol extract solution.

S.N.	Phytochemicals	Methanol Extract
1.	Alkaloids	+
2.	Flavonoids	+
3.	Glycosides	+
4.	Polyphenols	++
5.	Terpenoids.	+
6.	Saponins	+
7.	Quinones	+

+ = Presence, ++ = High Presence, - = Absence

FTIR Spectrum Analysis

The spectrum of FTIR provides information about the molecular structure and conformation of organic molecules as well as different functional groups present in the sample. The stretching frequency of the Carbon-heteroatom bond appeared in the FTIR spectrum is useful to identify it.

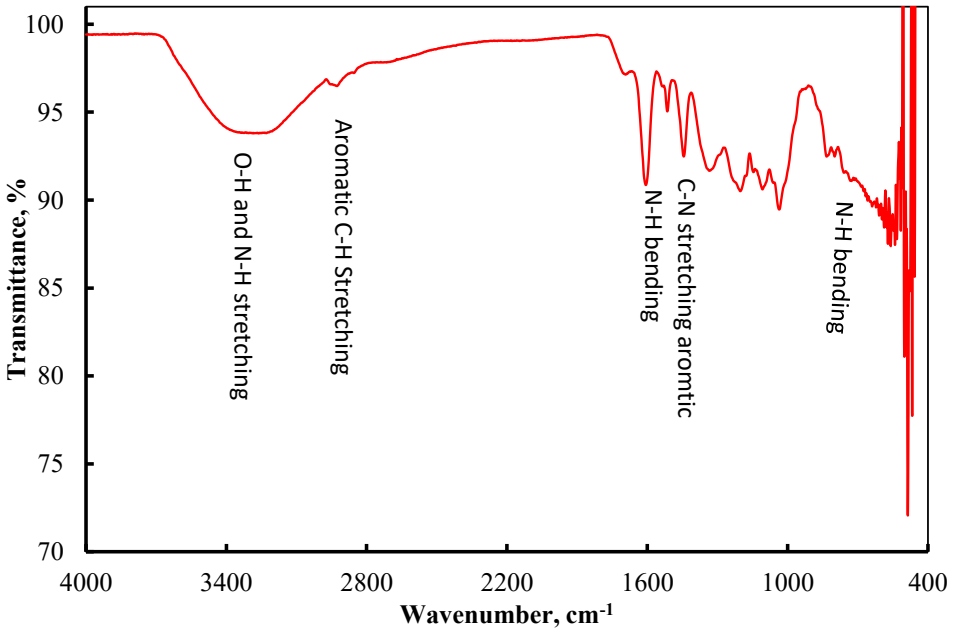

Fig 1. FTIR spectrum of bark extract of *S. robusta.*

The broad absorption band at 3200-3400 cm^{-1} is due to O-H stretching and N-H stretching of secondary amine (Figure 1). The sharp absorbance band at 2958 cm^{-1} is due to the aromatic C- H stretching of alkane and the splitting peak at 2851 cm^{-1} is due to the C-H stretching of the aldehyde group. The strong band at 1615 cm^{-1} is due to C=O stretching of the amide group and the band at 1519 cm^{-1} is due to N-H bending of amine. The medium absorbance band at 1357.88 cm^{-1} is due to the bending vibration of O-H bending of alcohol. Similarly, the absorption band at 1451 cm^{-1} is due to the C-N stretching of aromatic amine, absorption at 836 cm^{1} is due to N-H bending which corresponds to primary and secondary amines [13,42].

UV-Vis Spectra Analysis

The UV measurement is carried out for the identification of unsaturation or the presence of lone pair of electrons in the organic compounds. The UV spectra of methanol extract have been recorded and are shown in figure 2.

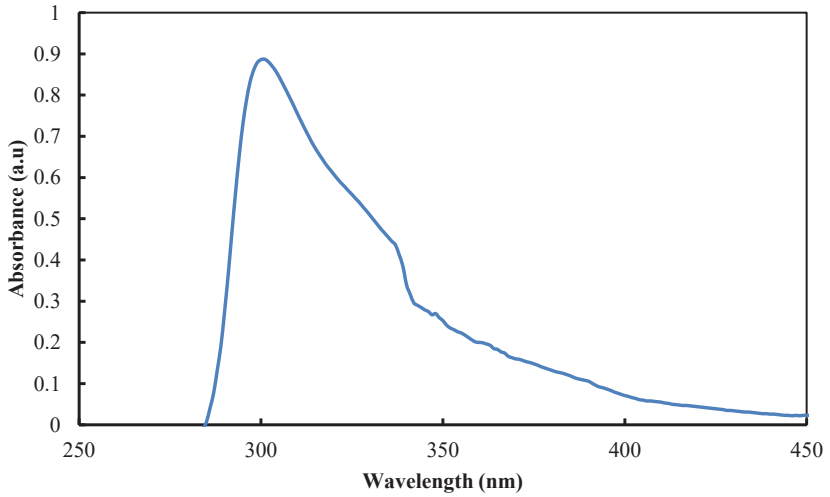

Fig 2. UV-Visible spectrum of methanol extract of *S. robusta* bark

The absorption of electromagnetic radiation was divided into near ultraviolet when absorption takes place at (200 nm to 380 nm) and it is mostly due to π-π* transition. The UV/Vis spectra of polyphenols are generally attributed to electronic transitions between p-type molecular orbitals (MOs), which are more or less extended over the molecular backbone, depending on the subclass as defined above (Figure 2). The given spectra of the methanol extract were found to be 301 nm with absorption of 0.887 a. u. This is also due to π-π* transition of organic compounds [42,43].

Morphological Study

Morphological characterization of the polished MS (Fresh and Immersed) was carried out by taking optical microscopic (OM) image. Images were captured by high performance microscope (Radical Scientific, RXLr-4) in Prof. Yadav's Laboratory, Central Department of Chemistry, TU, Kirtipur. The optical images of polished MS surfaces as well as the polished MS that are dipped in corrosive medium in the absence and presence of inhibitor are shown in figure 3 (a), 3(b) and 3(c), respectively. It is obvious that the polished surface of the MS is clear and smooth with no any corrosion products as shown in figure 3 a). Whereas the MS that dipped in corrosive medium in absence of inhibitor is greatly affected that resulted the formation of corrosion products. Small pits and rusts on the MS surface were observed as shown in figure 3(b). But, the surface of MS dipped in corrosive medium in presence of inhibitor is very interesting. Its surface was found to be smooth with very fine grey-green spots as in the figure 3 (c). These grey-green spots could be due to the adsorbed inhibitor molecules. Besides these, no any pits, grooves and corrosion products are seen. This indicated the inhibition behavior of inhibitor by the process of adsorption [1,13].

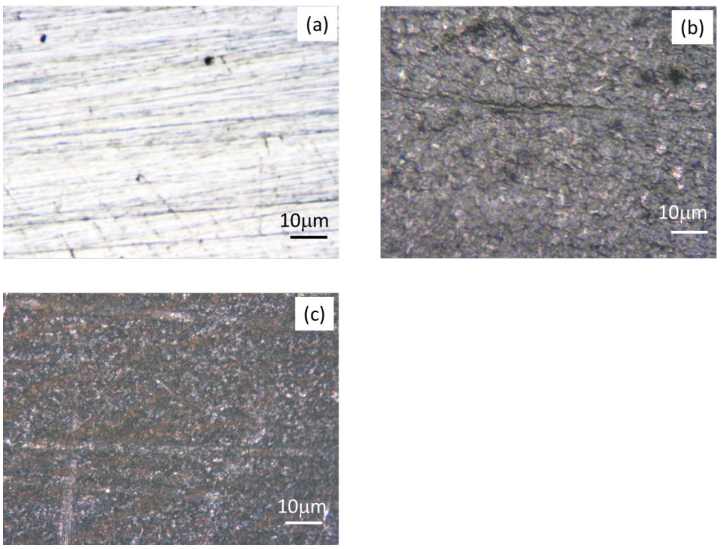

Fig 3. The MS surface images(a) Polished surface before immersion, (b) After 1 h dipping in acid at 25 °C , (c) After 1 h dipping in 1000 ppm inhibitor solution at 25 °C

Weight loss Measurement

Addition of inhibitor to the aggressive environment reduces the weight loss. When MS coupons are dipped in the aggressive solution, the interaction with the aggressive environment takes place resulting in the formation of corrosion products. After the formation of the corrosion product, the weight of MS gets decreased. Nature of the MS surface, working temperature and inhibitor concentration is responsible for the decrease in the weight of MS coupons. The loss in weight of MS could be high in absence of an inhibitor and gradually decreases with an increase in inhibitor concentration. Effect of working temperature, immersion time and inhibitor concentration for corrosion inhibition was monitored by weight loss measurement method.

Effect of Immersion Time

Effect of immersion time for corrosion inhibition was studied by measuring the weight loss of MS dipped in bare acid and inhibitor acid solution. The experiments were performed in different time intervals i.e. 1/2, 1, 3, 6, and 24 h. The weight loss data reflected that the presence of inhibitor reduces formation of corrosion product as compared to bare acid solution. The observed weight loss data at different immersion times are shown in figure 4.

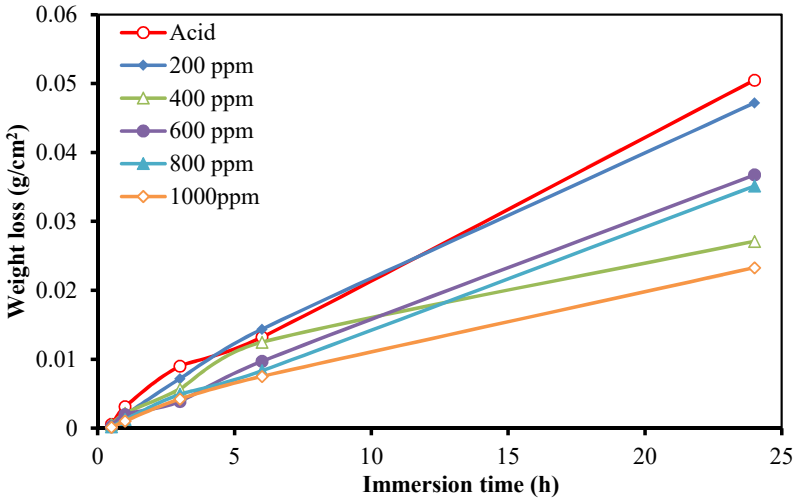

Fig 4. Weight loss of MS in different concentrations of inhibitor at temperature 18 °C.

It is found that due to the formation of inhibitor layer as barrier on the MS surface, weight of MS coupons decreased significantly as the concentration of inhibitor increased. Experimentally obtained values are shown in figure 5. The data reveals that the inhibition efficiency of the inhibitor below 6 h immersion is good, however there is highly decline in the efficiency. The decline on the efficiency at prolonged immersion time may have two reasons: desorption of inhibitor molecules from MS surface, and formation of chelate complex by inhibitor with free Fe^{2+} [36].

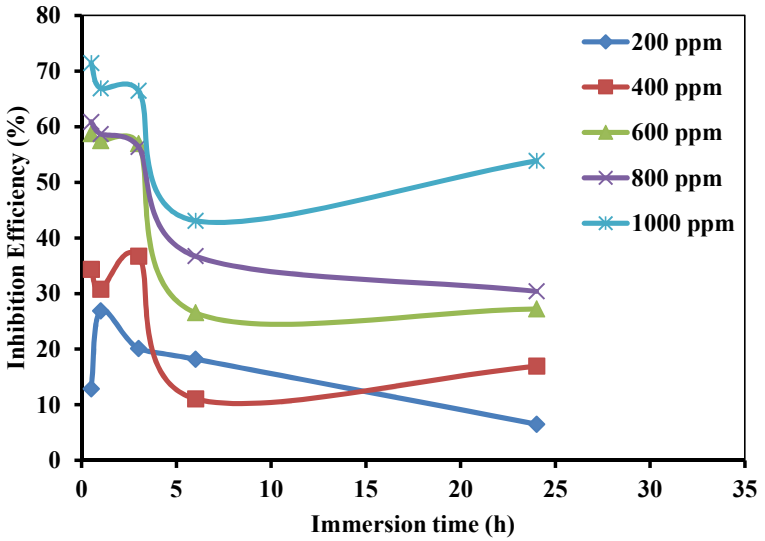

Fig 5. Variation of inhibition efficiency of the inhibitor for MS corrosion in 1M H_2SO_4 solution at different immersion time.

Effect of Inhibitor Concentration

Inhibitor concentration has great role in the corrosion inhibition process. In order to optimize the inhibitor concentration, weight loss measurement was carried out by dipping MS sample in the different concentrations (0, 200, 400, 600, 800, 1000 ppm) of inhibitors in 1M H_2SO_4 and bare acid solution. It is obvious that the weight loss of MS in bare acid is very high in comparison to loss in inhibitor solution. The weight loss data indicates that the inhibition efficiency increases as the increase in concentration. It is because, at higher concentrations, a large number of molecules are available for adsorption onto the MS surface. The maximum inhibition efficiency was found to be 71.47% at 0.5 h immersion time in 1000 ppm inhibitor concentration. This efficiency didn't remain constant on increasing immersion time. The minimum efficiency of 1000 ppm inhibitor concentration was found to be 43.1% at 6 hours (Figure 6).

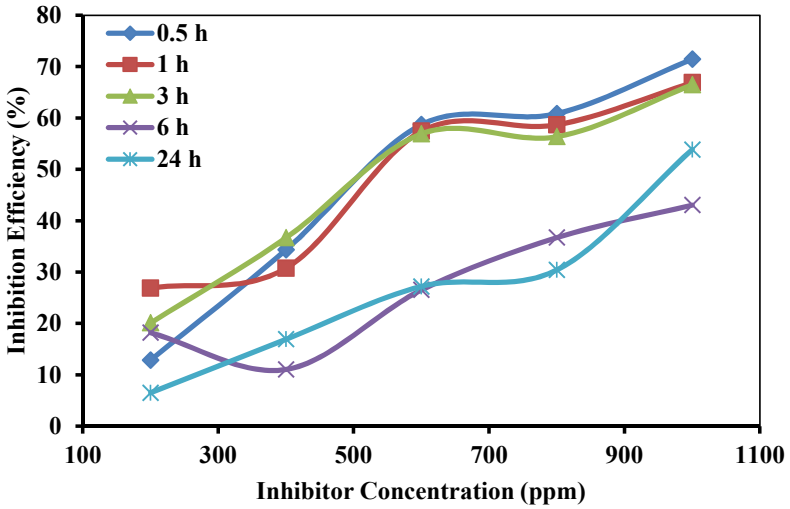

Fig 6. Variation in the inhibition efficiency of the inhibitor with concentration at different immersion time.

Effect of Working Temperature

The effect of working temperature on the corrosion inhibition was studied in the inhibitor solutions of different concentrations (200, 400, 600, 800 & 1000 ppm). The weight loss of MS coupon dipped in the inhibitor solution of different concentration was measured in the reference of acid solution. Working temperature effect was studied by immersing MS coupons in the inhibitor and acid solutions separately for one hour at different temperatures (18, 28, 38, 48 & 58 °C).

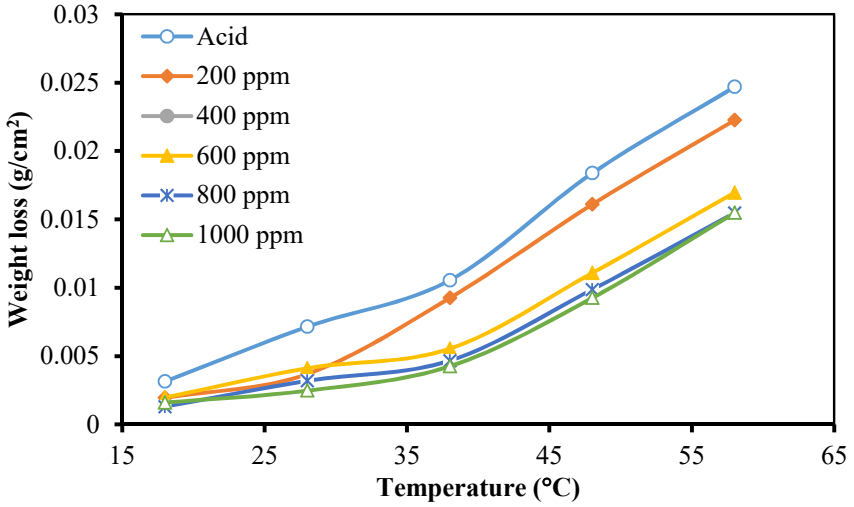

Fig 7. Variation of weight loss of MS with temperature in the presence and absence of inhibitor.

The variation of weight of MS in different concentrations of inhibitor with temperature is shown in figure 7. In the graph, it is clear that the weight of MS was increased gradually with increasing temperature, it is because the hydrogen evolution reaction takes place so rapidly at increasing activation energy with higher temperature. The weight loss of MS dipped in acid only solution is very high. But, the weight loss of the MS gradually decreases up on increasing the inhibitor concentration.

It is clear that the inhibition efficiency is maximum at 28 °C where the maximum efficiency of 65.3% at 1000 ppm inhibitor concentration was observed (Figure 8). It was very interesting that the methanol extract of *S. Robusta* was not decomposed even at 50 °C temperature. So it can be claimed that the 1000 ppm methanol extract prepared from *S. Robusta* can work at higher temperatures up to 48-50 °C. Above this temperature, the structural deformation of molecules as well as desorption of molecules from MS surface may occur which leads to the decrease in inhibition efficiency.

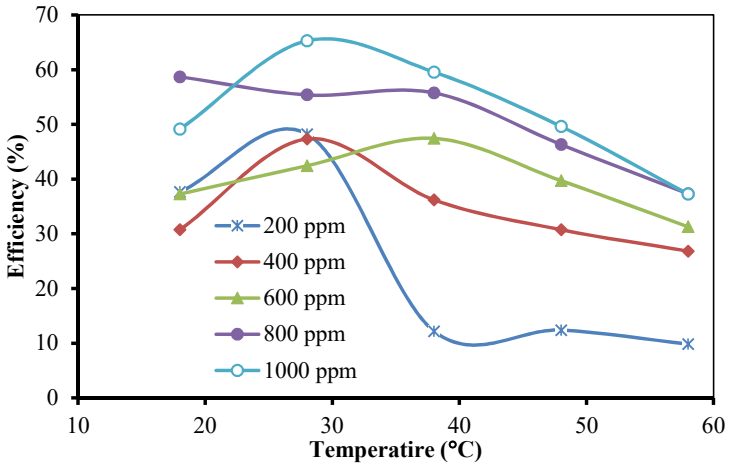

Fig 8. Variation of Inhibition efficiency with temperature by different concentrations of methanol extract in 1M H_2SO_4.

Activation Energy

The activation energy of the reaction in the acid only and inhibitor solutions in a corrosion cell can be explained by plotting a graph between logarithms of the rate of corrosion to 1/2.303RT . Activation energy was calculated from slope of the straight line [10,44] and found to be 40.72 kJ/mol for the reaction between MS surface and acid molecules.

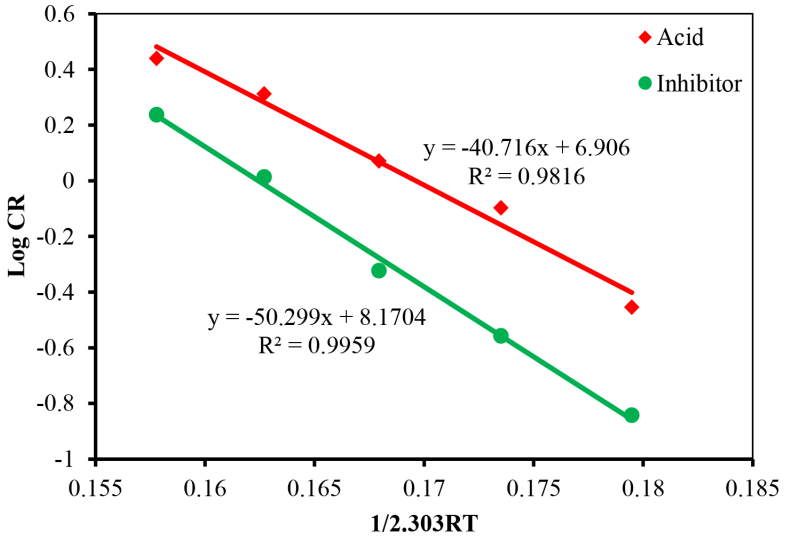

Fig 9. Arrhenius plot for MS in 1M H_2SO_4 with and without inhibitor.

But, in presence of inhibitor, the energy of activation increased to 50.29 kJ/mol for 1000 ppm inhibitor solution as shown in figure 9. From these finding it can be claimed that the corrosion rate is decreased by suppressing the chemical reaction between acid and MS surface. The activation energy of the system is found to be less than 80 kJ/mol. This substantiates the physisorption of inhibitor molecules on MS surface [45,46].

Enthalpy and Entropy Measurement

The enthalpy and entropy of the corrosion system was calculated by using the transition state equation by plotting a graph between log (CR/T) against 1/2.303RT. Transition enthalpy (ΔH°) was determined from the slope the of straight line and that of transition entropy (ΔS°) was calculated from intercept value [10,47].

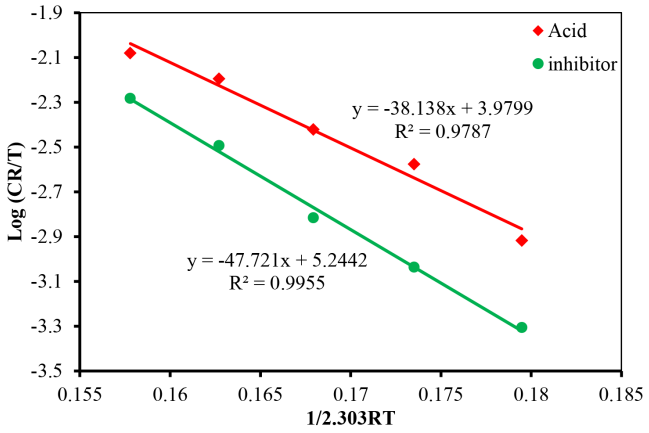

Fig 10. Transition state plot for MS in 1M H_2SO_4 with and without inhibitor.

From the transition state plot (figure 10), the enthalpy of the system in the absence of an inhibitor was found to be 38.14 kJ/mol. But, it was increased to 47.72 kJ/mol in 1000 ppm inhibitor solution. The transition enthalpy of the system is found to be positive indicating the endothermic adsorption process [48]. The transition enthalpy is increased upon addition of inhibitor in the acid solution. This indicates the kinetic control of corrosion rate [49]. As the transition enthalpy value is smaller than activation energy implies the hydrogen evolution process leading the reduction of total reaction volume has been observed [50,51].

This increase in transition enthalpy indicates a decrease in the corrosion rate. The transition entropy of this system has been calculated from the intercept and found to be -121.411 and -86.175 $JK^{-1}mol^{-1}$ for acid and 1000 ppm inhibitor solutions, respectively. Very fascinatingly, increasing transition state entropy of the system is due to the increased density of proton roaming in the solution as well as quasi-substitution process [2,37]. These values of E_a, $\Delta H°$ and $\Delta S°$ support the adsorption behavior of the inhibitor on the metal surface (Table 3). The presence of an inhibitor increases the activation energy and reduces the reaction rate. In addition, this increase in activation energy indicates the adsorption of inhibitor molecules on the MS surface or coverage of the metal surface by forming a barrier [10,52].

Table 3. Activation parameters of the MS dissolution in 1 M H_2SO_4 without and with inhibitor.

Corrosive environment	E_a (kJ/mol)	$\Delta H°$ (kJ/mol)	Ea-ΔH=RT	$\Delta S°$ ($JK^{-1}mol^{-1}$)
1M Sulfuric Acid	40.72	38.14	2.58	-121.411
1000 ppm inhibitor	50.29	47.72	2.57	-97.122

Electrochemical Performances

Open circuit potential (OCP) measurement is one of the simplest method for indirect corrosion monitoring technique. To attain equilibrium before polarization, OCP was monitored for 30 minutes at laboratory (27 °C) temperature for MS dipped in both acid and inhibitor solution. OCP of the samples for immersed and as-immersed condition are shown in figure 11 and 12.

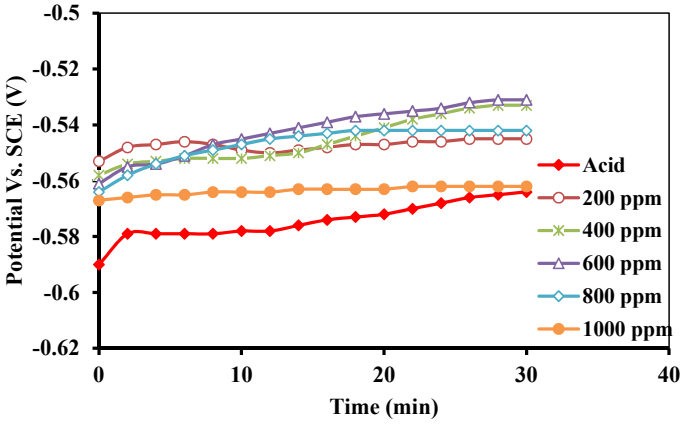

Fig 11. Variation of OCP with the time of immersion of mild steel in different concentrations of inhibitor in 1M H_2SO_4 measured at the time of immersion.

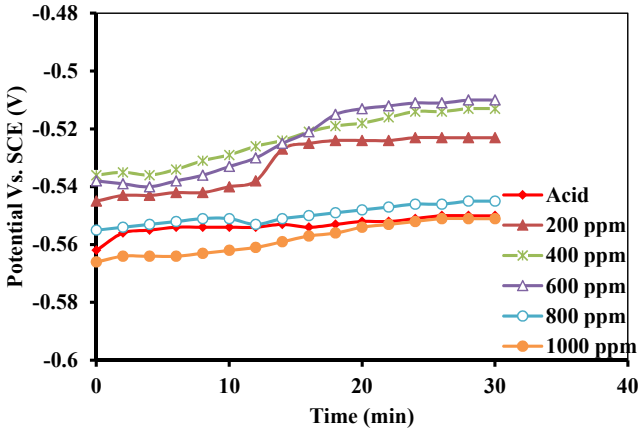

Fig 12. Variation of OCP with the time of immersion of mild steel in different concentrations of inhibitor in 1M H_2SO_4 measured after 1 h immersion in solutions.

Initially, the potential shifted to more positive, but the shift in the value of OCP is less than 50 mV, in both immersed and as-immersed condition, indicating plant extract act as a mixed corrosion inhibitor. The shifting of potential from OCP to more positive indicates the formation of a protective layer by inhibitor molecules in acid solution on the MS surface, (i.e. Passivation) that limits the interaction of aggressive ions with the MS surface [1,13,44].

After equilibrium, the polarization measurement was carried out for all the samples dipped in acid and inhibitor solutions for both as-immersed and immersed condition. Polarization was performed by applying ±350 mV potential from OCP.

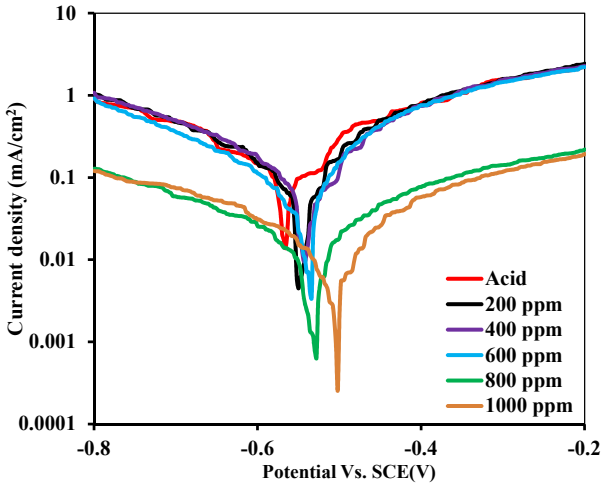

Fig 13. Potentiodynamic polarization curves for mild steel in 1M H_2SO_4 containing different concentrations of inhibitor as-immersed condition.

The results displayed in the table 4, indicates that the corrosion current density is in the descending order with the ascending order of inhibitor concentration. This could be due the blockage of reacting sites by inhibitor molecules.

Table 4. Anodic and cathodic slope and inhibition efficiency for as-immersed sample.

Medium	OCP	Icorr	Anodic slope	Cathodic slope	Efficiency (%)
Acid	-0.568	0.102	10.96	-4.02	-
200 ppm	-0.55	0.073	16.46	-7.76	28.4314
400 ppm	-0.548	0.063	15.34	-6.18	38.2353
600 ppm	-0.528	0.03	10.18	-10.02	70.5882
800 ppm	-0.548	0.0094	8.56	-4.49	90.7843
1000 ppm	-0.502	0.0064	9.22	-6.25	93.7255

Polarization measurement was carried out in the MS coupons dipped for 1 h in the acid and inhibitor solutions and presented in Figure 14. The results reveal that the current density found to be decreased as the inhibitor concentration increased. It is because of the resistance of inhibitor solution toward corrosion reaction due to MS surface coverage by inhibitor molecules. The inhibitor efficiency, cathodic and anodic slope, OCP and corrosion current densities obtained from polarization are tabulated in table 4.

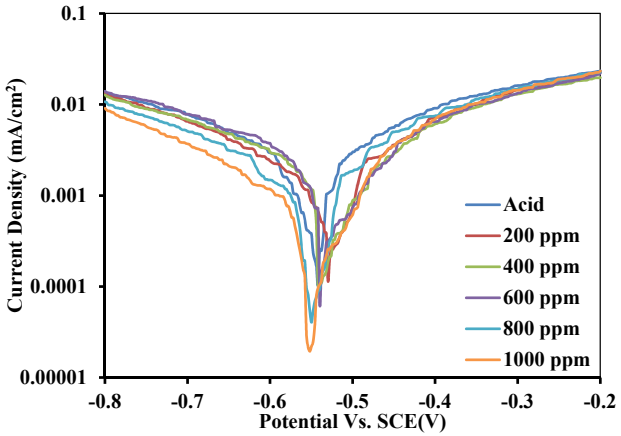

Fig 14. Potentiodynamic polarization curves for mild steel in 1M H_2SO_4 containing different concentrations of inhibitor immersed condition.

Table 5. Table showing the anodic and cathodic slope and inhibition efficiency for immersed sample.

Medium	OCP	Icorr	Anodic slope	Cathodic slope	Efficiency (%)
Acid	-0.542	0.001	6.89	-5.04	-
200 ppm	-0.53	0.00088	8.75	-4.89	12
400 ppm	-0.542	0.0007	12.5	-4.28	30
600 ppm	-0.54	0.00054	12.59	-4.2	46
800 ppm	-0.55	0.00046	10	-5.09	54
1000 ppm	-0.552	0.00025	15.8	-4.11	75

Anodic and cathodic slopes for each polarization curves are tabulated in table 4 and 5. The anodic and cathodic slopes give the information regarding the mechanism of corrosion inhibition. The trend of anodic and cathodic slopes has not been changed. This indicates that the mechanism/ or corrosion inhibition pathway has not been changed. It also can be stated that up on increment of inhibitor concentration, the inhibition efficacy has been increased but the pathway to control corrosion rate has not been changed.

Inhibition efficiency obtained by polarization measurement for both immersed and as-immersed samples in varying concentrations are presented in figure 15. It reveals that the inhibition efficiency increases with an increase in the concentration of the inhibitor solution. This is due to the increase in the fraction of surfaces covered by inhibitor molecules. The maximum efficiency was found as 93.73% and 75% at 1000 ppm concentration of the inhibitor solution in 1M H_2SO_4 on MS sample as-immersed and immersed for 1 hour respectively.

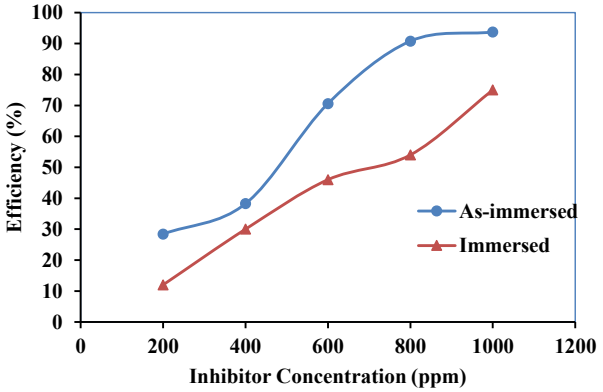

Fig 15. Inhibition efficiency of inhibitor obtained from the polarization of both immersed and as-immersed MS sample 1M H_2SO_4 in the presence and absence of inhibitor.

Mechanism of Corrosion Inhibition

Corrosion inhibition by green inhibitors occurs by adsorption mechanism. However, the adsorption process is not simple. The activation energy value supports the physical adsorption and spontaneous process. The slopes of the polarization curves are in same trend indicated the adsorption pathway has not been changed. The corrosion rate has been controlled by blocking both anodic and cathodic reactions simultaneously. Corrosion inhibition by inhibitor molecules is due to the adsorption of inhibitor molecules on the MS surface by the replacement of water molecules, called the quasi-substitution process.

In (sol) + xH_2O (ads) === In (ads) + H_2O (sol)

Where, In (sol) and In (ads) represent the solvated and adsorbed inhibitor molecules, respectively. Similarly, H_2O (ads) represents the adsorbed water molecules on the MS surface, and x represents the size ratio i.e. many water molecules that are replaced by one organic molecule [25].

OCP gives the information where there is a positively or negatively charged MS surface. The OCP of MS is recorded at around -0.56 V, which is more positive than PZC value. It implies that the surface of the metal is positively charged in the inhibitor solution [25,36]. In a positively charged surface, there could be an interaction of SO_4^{2-} ions and the surface becomes negatively charged. The protonated inhibitor molecules interact with sulfate ions by the electrostatic force of attraction. The protonated inhibitor molecules return to their neutral form after releasing H_2 molecules [36,53]. Then, the electron pair of HOMO with a high electron density of inhibitor molecules is shared with the vacant d-orbital of iron and forms a coordinate covalent bond. This accumulates the extra negative charge on the MS surface. To relive the charge, electrons are returned to LUMO with high orbital density especially to antibonding π^* orbital of the organic molecule [13,36,53].

Conclusions

Methanol extract was prepared from the bark of *S. robusta*. The chemical and spectroscopic characterization of the extract was carried out and the results obtained from these evaluations reflected the possible active centers in the extract for adsorption. Corrosion kinetics and the thermodynamics were evaluated. The activation energy, enthalpy and entropy values obtained in the process indicated the adsorption of inhibitor molecules on the MS surface or coverage of the metal surface by forming a barrier. Electrochemical characterization reflects the mixed type of inhibition by extract, with the maximum efficiency 93.73% and 75% in the 1000 ppm of inhibitor solution, respectively for the as-immersed and the immersed samples. This inhibitor could be used for short period of immersion.

Acknowledgements

Authors are grateful to the Department of Chemistry, Amrit Campus, for laboratory as well chemical support, Central Department of Chemistry for electrochemical characterization, and Province Planning Commission, Lumbini for financial support (2078/079 Project).

References

1. D. Parajuli, S. Sharma, H.B. Oli, D.S. Bohara, D.P. Bhattarai, A.P. Tiwari, A.P. Yadav. Comparative Study of Corrosion Inhibition Efficacy of Alkaloid Extract of *Artemesia vulgaris* and *Solanum tuberosum* in Mild Steel Samples in 1 M Sulphuric Acid, *Electrochem,* (2022), *3*, 416–433.
2. H.B. Oli, J. Thapa Magar, N. Khadka, A. Subedee, D.P. Bhattarai, B. Pant. *Coriaria nepalensis* Stem Alkaloid as a Green Inhibitor for Mild Steel Corrosion in 1 M H_2SO_4 Solution, *Electrochem,* (2022), *3*, 713–727.
3. S.S. Al-Shihry, A.R. Sayed, H.M. Abd El-lateef. Design and Assessment of a Novel Poly (Urethane-Semicarbazides) Containing Thiadiazoles on the Backbone of the Polymers as Inhibitors for Steel Pipelines Corrosion in CO_2-Saturated Oilfield Water, *Journal of Molecular Structure,* (2020), *1201*, 127223.
4. C. Garcia-Cabezon, C. Salvo-Comino, C. Garcia-Hernandez, M.L. Rodriguez-Mendez, F. Martin-Pedrosa. Nanocomposites of Conductive Polymers and Nanoparticles Deposited on Porous Material as a Strategy to Improve Its Corrosion Resistance, *Surface and Coatings Technology,* (2020), *403*, 126395.

5. D.K. Gupta, S. Neupane, S. Singh, N. Karki, A.P. Yadav. The Effect of Electrolytes on the Coating of Polyaniline on Mild Steel by Electrochemical Methods and Its Corrosion Behavior, *Progress in Organic Coatings,* (2021), *152*, 106127.
6. N. Gladkikh, Y. Makarychev, M. Maleeva, M. Petrunin, L. Maksaeva, A. Rybkina, A. Marshakov, Y. Kuznetsov. Synthesis of Thin Organic Layers Containing Silane Coupling Agents and Azole on the Surface of Mild Steel: Synergism of Inhibitors for Corrosion Protection of Underground Pipelines, *Progress in Organic Coatings,* (2019), *132*, 481–489.
7. K. Sayin, D. Karakaş. Quantum Chemical Studies on the Some Inorganic Corrosion Inhibitors, *Corrosion science,* (2013), *77*, 37–45.
8. N. Arshad, A.K. Singh, B. Chugh, M. Akram, F. Perveen, I. Rasheed, F. Altaf, P.A. Channar, A. Saeed. Experimental, Theoretical, and Surface Study for Corrosion Inhibition of Mild Steel in 1 M HCl by Using Synthetic Anti-Biotic Derivatives, *Ionics,* (2019), *25*, 5057–5075.
9. S. Umoren, O. Ogbobe, I. Igwe, E. Ebenso. Inhibition of Mild Steel Corrosion in Acidic Medium Using Synthetic and Naturally Occurring Polymers and Synergistic Halide Additives, *Corrosion science,* (2008), *50*, 1998–2006.
10. N. Karki, Y. Choudhary, A.P. Yadav. Thermodynamic, Adsorption and Corrosion Inhibition Studies of Mild Steel by *Artemisia vulgaris* Extract from Methanol as Green Corrosion Inhibitor in Acid Medium, *Journal of Nepal Chemical Society,* (2018), *39*, 76–85.
11. H.J. Li, W. Zhang, Y.C. Wu. Anti-Corrosive Properties of Alkaloids on Metals, In *Alkaloids-Their Importance in Nature and Human Life*, Intech Open, 2018, ISBN 1-78984-577-7.
12. O. Fayomi, I. Akande, U. Nsikak. An Overview of Corrosion Inhibition Using Green and Drug Inhibitors, IOP Publishing, 2019, 1378, p 022022.
13. A. Chapagain, D. Acharya, A.K. Das, K. Chhetri, H.B. Oli, A.P. Yadav. Alkaloid of *Rhynchostylis retusa* as Green Inhibitor for Mild Steel Corrosion in 1 M H_2SO_4 Solution, *Electrochem,* (2022), *3*, 211–224.
14. M. Finšgar, J. Jackson. Application of Corrosion Inhibitors for Steels in Acidic Media for the Oil and Gas Industry: A Review, *Corrosion science,* (2014), *86*, 17–41.
15. J.O. Mendes, E.C. da Silva, A.B. Rocha. On the Nature of Inhibition Performance of Imidazole on Iron Surface, *Corrosion science,* (2012), *57*, 254–259.
16. M. Ramezanzadeh, G. Bahlakeh, Z. Sanaei, B. Ramezanzadeh. Studying the *Urtica dioica* Leaves Extract Inhibition Effect on the Mild Steel Corrosion in 1 M HCl Solution: Complementary Experimental, Ab Initio Quantum Mechanics, Monte Carlo and Molecular Dynamics Studies, *Journal of Molecular Liquids,* (2018), *272*, 120–136.
17. C.C. Aralu, H.O. Chukwuemeka-Okorie, K.G. Akpomie. Inhibition and Adsorption Potentials of Mild Steel Corrosion Using Methanol Extract of *Gongronema latifoliuim*, *Applied Water Science,* (2021), *11*, 1–7.
18. P.R. Shrestha, H.B. Oli, B. Thapa, Y. Chaudhary, D.K. Gupta, A.K. Das, K.B. Nakarmi, S. Singh, N. Karki, A.P. Yadav. Bark Extract of Lantana Camara in 1M HCl as Green Corrosion Inhibitor for Mild Steel, *Engineering Journal,* 2019, *23*, 205–211.
19. A. Berrissoul, A. Ouarhach, F. Benhiba, A. Romane, A. Zarrouk, A. Guenbour, B. Dikici, A. Dafali. Evaluation of *Lavandula mairei* Extract as Green Inhibitor for Mild Steel Corrosion in 1 M HCl Solution. Experimental and Theoretical Approach, *Journal of Molecular Liquids,* (2020), *313*, 113493.
20. M. Rana, S. Joshi, J. Bhattarai. Extract of Different Plants of Nepalese Origin as Green Corrosion Inhibitor for Mild Steel in 0.5 M NaCl Solution, *Asian Journal of Chemistry,* (2017), *29*, 1130.
21. L. Yahaya, S. Aroyeun, S. Ogunwolu, C. Jayeola, R. Igbinadolor. Green and Black Tea (*Camellia sinensis*) Extracts as Corrosion Inhibitor for Mild Steel in Acid Medium, *World Applied Sciences Journal,* (2017), *35*, 985–992.
22. L.A. Nnanna, K.O. Uchendu, F.O. Nwosu, U. Ihekoronye, P. Eti. *Gmelina arborea* Bark Extracts as a Corrosion Inhibitor for Mild Steel in an Acidic Environment, *International Journal Material Chemistry,* (2014), *4*, 34–39.
23. P. Muthukrishnan, B. Jeyaprabha, P. Prakash. Mild Steel Corrosion Inhibition by Aqueous Extract of *Hyptis suaveolens* Leaves, *International Journal of Industrial Chemistry,* (2014), *5*, 1–11.

24. N. Mathur, R. Chhipa. Study of Corrosion Inhibitors (*Pennisetum glaucum*) Extracts on Mild Steel Used in Building Construction, *International Journal of Engineering Science Research and Technology,* (2014), *3*, 845.
25. N. Karki, S. Neupane, D.K. Gupta, A.K. Das, S. Singh, G.M. Koju, Y. Chaudhary, A.P. Yadav. Berberine Isolated from *Mahonia nepalensis* as an Eco-Friendly and Thermally Stable Corrosion Inhibitor for Mild Steel in Acid Medium, *Arabian Journal of Chemistry,* (2021), *14*, 103423.
26. N. Karki, S. Neupane, Y. Chaudhary, D. Gupta, A.P. Yadav. *Equisetum hyemale*: A New Candidate for Green Corrosion Inhibitor Family, *International Journal of Corrosion and Scale Inhibition,* (2021), *10*, 206–227.
27. C. Kamal, M.G. Sethuraman, A. Caulerpin. Bis-Indole Alkaloid as a Green Inhibitor for the Corrosion of Mild Steel in 1 M HCl Solution from the Marine Alga *Caulerpa racemosa*, *Industrial & Engineering Chemistry Research,* (2012), *51*, 10399–10407.
28. P.B. Raja, M. Fadaeinasab, A.K. Qureshi, A.A. Rahim, H. Osman, M. Litaudon, K. Awang. Evaluation of Green Corrosion Inhibition by Alkaloid Extracts of *Ochrosia oppositifolia* and Isoreserpiline against Mild Steel in 1 M HCl Medium, *Industrial & Engineering Chemistry Research,* (2013), *52*, 10582–10593.
29. P.B. Raja, A.K. Qureshi, A.A. Rahim, H. Osman, K. Awang. *Neolamarckia cadamba* Alkaloids as Eco-Friendly Corrosion Inhibitors for Mild Steel in 1 M HCl Media, *Corrosion Science,* (2013), *69*, 292–301.
30. A. Ikeuba, P. Okafor, U. Ekpe, E.E. Ebenso. Alkaloid and Non-Alkaloid Ethanolic Extracts from Seeds of *Garcinia kola* as Green Corrosion Inhibitors of Mild Steel in H_2SO_4 Solution, *International Journal of Electrochemical Science,* (2013), *8*, 7455–7467.
31. B.U. Ugi. Alkaloid and Non Alkaloid Extracts of *Solanum melongena* Leaves as Green Corrosion Inhibitors on Carbon Steel in Alkaline Medium, *Fountain Journal of Natural and Applied Sciences,* (2014), *3*, 1-9.
32. M. Faustin, A. Maciuk, P. Salvin, C. Roos, M. Lebrini. Corrosion Inhibition of C38 Steel by Alkaloids Extract of *Geissospermum* Laeve in 1 M Hydrochloric Acid: Electrochemical and Phytochemical Studies, *Corrosion Science,* (2015), *92*, 287–300.
33. N. El Hamdani, R. Fdil, M. Tourabi, C. Jama, F. Bentiss. Alkaloids Extract of *Retama monosperma* (L.) Boiss. Seeds Used as Novel Eco-Friendly Inhibitor for Carbon Steel Corrosion in 1 M HCl Solution: Electrochemical and Surface Studies, *Applied Surface Science,* (2015), *357*, 1294–1305.
34. B. Ngouné, M. Pengou, A.M. Nouteza, C.P. Nanseu-Njiki, E. Ngameni. Performances of Alkaloid Extract from *Rauvolfia macrophylla* Staph toward Corrosion Inhibition of C38 Steel in Acidic Media, *ACS omega,* (2019), *4*, 9081– 9091.
35. K. Sadik, N.E. Hamdani, M. Hachim, S. Byadi, I. Bahadur, A. Aboulmouhajir. Towards a Theoretical Understanding of Alkaloid-Extract Cytisine Derivatives of *Retama monosperma* (L.) Boiss. Seeds, as Eco-Friendly Inhibitor for Carbon Steel Corrosion in Acidic 1M HCl Solution, *Journal of Theoretical and Computational Chemistry,* (2020), *19*, 2050013.
36. K. Dhakal, D.S. Bohara, B.B. Bist, H.B. Oli, D.P. Bhattarai, S. Singh, N. Karki, A.P. Yadav. Alkaloids Extract of *Alnus nepalensis* Bark as a Green Inhibitor for Mild Steel Corrosion in 1 M H_2SO_4 Solution, *Journal of Nepal Chemical Society,* (2022), *43*, 76–92, doi:https://doi.org/10.3126/jncs.v43i1.46999.
37. R. Karki, A.K. Bajgai, N. Khadka, O. Thapa, T. Mukhiya, H.B. Oli, D.P. Bhattarai, *Acacia catechu* Bark Alkaloids as Novel Green Inhibitors for Mild Steel Corrosion in a One Molar Sulphuric Acid Solution, *Electrochem,* (2022), *3*, 668–687, doi:https://doi.org/10.3390/electrochem3040044.
38. O. Thapa, J. Thapa Magar, H.B. Oli, A. Rajaure, D. Nepali, D.P. Bhattarai, T. Mukhiya. Alkaloids of *Solanum xanthocarpum* Stem as Green Inhibitor for Mild Steel Corrosion in One Molar Sulphuric Acid Solution, *Electrochem,* (2022), *3*, 820-842.
39. N. Timilsina, M.S. Ross, J.T. Heinen. A Community Analysis of Sal (*Shorea robusta*) Forests in the Western Terai of Nepal, *Forest Ecology and Management,* (2007), *241*, 223–234.
40. A. Kalaiselvan, K. Gokulakrishnan, T. Anand, U. Akhilesh, S. Velavan. Preventive Effect of *Shorea robusta* Bark Extract against Diethylnitrosamine-Induced Hepatocellular Carcinoma in Rats, *International Research Journal of Medical Science,* (2013), *1*, 2–9.

41. R.K. Soni, V. Dixit, R. Irchhaiya, H. Singh. A Review Update on *Shorea robusta* Gaertn f.(Sal), *Journal of Drug Delivery & Therapeutics,* (2013), *3*, 127–132.
42. R.M. Silverstein, G.C. Bassler. Spectrometric Identification of Organic Compounds, *Journal of Chemical Education,* (1962), *39*, 546.
43. H.B. Oli, N. Sharma, E. K.C., A. Subedee, R. Timilsina. Green Synthesis of Copper Nanoparticles Using *Zingiber officinale* Extract and Characterization, *Journal of Nepal Chemical Society,* (2018), *39*, 10–17.
44. G. Ijuo, H. Chahul, I. Eneji. Kinetic and Thermodynamic Studies of Corrosion Inhibition of Mild Steel Using *Bridelia ferruginea* Extract in Acidic Environment, *Journal of Advanced Electrochemistry,* (2016), *2*, 107–112.
45. V.J. Inglezakis, A.A. Zorpas. Heat of Adsorption, Adsorption Energy and Activation Energy in Adsorption and Ion Exchange Systems, *Desalination and water treatment,* (2012), *39*, 149–157.
46. N. Gopal, M. Asaithambi. Adsorption of Acid Blue-40 (A Textile Dye) Using *Prosopis juliflora* Activated Carbon Embedded in Polyaniline Matrix, *Rasayan Journal of Chemistry,* (2015), *8*, 279–286.
47. H.B. Oli, D.L. Parajuli, S. Sharma, A. Chapagain, A.P. Yadav. Adsorption Isotherm and Activation Energy of Inhibition of Alkaloids on Mild Steel Surface in Acidic Medium, *Amrit Research Journal,* (2021), *2*, 59–67.
48. A.S. Yaro, A.A. Khadom, R.K. Wael. Apricot Juice as Green Corrosion Inhibitor of Mild Steel in Phosphoric Acid, *Alexandria Engineering Journal,* (2013), *52*, 129–135.
49. J.I. Bhat, V.D. Alva. Meclizine Hydrochloride as a Potential Non-Toxic Corrosion Inhibitor for Mild Steel in Hydrochloric Acid Medium, *Archives of Applied Science Research,* (2011), *3*, 343–356.
50. Y. Qiang, S. Zhang, B. Tan, S. Chen. Evaluation of Ginkgo Leaf Extract as an Eco-Friendly Corrosion Inhibitor of X70 Steel in HCl Solution, *Corrosion Science,* (2018), *133*, 6–16.
51. R.S. Erami, M. Amirnasr, S. Meghdadi, M. Talebian, H. Farrokhpour, K. Raeissi. Carboxamide Derivatives as New Corrosion Inhibitors for Mild Steel Protection in Hydrochloric Acid Solution, *Corrosion Science,* (2019), *151*, 190–197.
52. E. Ituen, O. Akaranta, A. James. Evaluation of Performance of Corrosion Inhibitors Using Adsorption Isotherm Models: An Overview, *Chemical Science International Journal,* (2017), *18*, 1–34.
53. N. Karki, S. Neupane, Y. Chaudhary, D.K. Gupta, A.P. Yadav. Berberis Aristata: A Highly Efficient and Thermally Stable Green Corrosion Inhibitor for Mild Steel in Acidic Medium, *Analytical and Bioanalytical Electrochemistry,* (2020), *12*, 970–988.